Structural and Photophysical Characterisation of *fac*-[Tricarbonyl(chloro)-(5,6-epoxy-1,10-phenanthroline)rhenium(I)]

Angel A. Martí,[a] Gellert Mezei,[a] Lorena Maldonado,[a] Giovanni Paralitici,[a] Raphael G. Raptis,[a] and Jorge L. Colón*[a]

Keywords: Carbonyl ligands / Coincidental resonances / Facial isomers / Energy gap law / Rhenium

The structural and spectroscopic characterisations of *fac*-[Re(phen)$(CO)_3$Cl] (**1**) (phen = 1,10-phenanthroline), *fac*-[Re(ephen)$(CO)_3$Cl] (**3**) [ephen = 5,6-epoxy-1,10-phenanthroline (**2**)] and ephen are reported. The appearance of weak hydrogen bond networks in the crystal lattice of [Re(ephen)$(CO)_3$Cl] and ephen are discussed. Two different isomers of [Re(ephen)$(CO)_3$Cl] were identified by IR and NMR spectroscopy. Coincidental resonances were differentiated for these complexes by temperature-dependent NMR spectroscopy. Recrystallisation of the crude material allowed the separation of the two isomers. The spectroscopic data permitted the calculation of radiative and nonradiative luminescence rate constants which are consistent with the energy gap law.

Introduction

The first observation of electronically excited luminescence in carbonylmetal compounds at room temperature was reported by Wrighton and Morse in 1974 for [ReX$(CO)_3$Cl], where X is 1,10-phenanthroline and its derivatives.[1] Since then, a great variety of luminescent carbonylmetal complexes have emerged with applications in areas ranging from electronic and energy transfer to catalysis.[2] In the last few years, self-assembled multinuclear carbonylrhenium complexes have been prepared with interesting photophysical and photochemical properties.[3] In addition, carbonylrhenium compounds have been used to modify proteins with the aim of studying biological electron transfer pathways.[4]

Tricarbonylrhenium(I) complexes are d^6 species which undergo spin-forbidden charge transfer emissions after photoexcitation.[5] Excitation promotes an electron from rhenium-centred orbitals to π* ligand localised orbitals, whereupon internal conversion occurs to the triplet state (or mixed singlet-triplet state) followed by subsequent relaxation into the ground state with the emission of a photon.[1] These d^6 complexes are isoelectronic with tris(2,2′-bipyridine)ruthenium(II) and their emission properties are similar to other d^6 metal complexes which undergo electron transfer reactions from their excited states.[6]

The construction of supramolecular assemblies of photoactive metal complexes requires the availability of well-characterised and preferably easily synthesised moieties with functionalities that allow their attachment to other parts of the framework. Among the possibilities, epoxy group containing molecules are good candidates because they enable the easy formation of covalent bonds between a carbon atom and a specific anchoring group. This possibility has been explored by Shen and Sullivan who used an epoxidised phenanthroline for the attachment of a crown ether.[7] The phenanthroline was then coordinated to a tricarbonylrhenium centre to complete the photoluminescent system. These authors reported that treatment of [Re$(CO)_5$Cl] with 5,6-epoxy-1,10-phenanthroline (ephen, **2**) produced *fac*-[tricarbonyl(chloro)(5,6-epoxy-1,10-phenanthroline)rhenium(I)] {*fac*-[Re(ephen)$(CO)_3$Cl], **3**}. However, no detailed synthetic scheme or characterisation of this complex was reported. As stated above, detailed structural and photophysical characterisation of this complex is necessary if the intention is to use it as part of photoactive molecular frameworks. Here, we report the complete structural and photophysical characterisation of *fac*-[Re(ephen)$(CO)_3$Cl]. In addition, for comparison, we have determined the crystal structure of *fac*-[tricarbonyl(chloro)(1,10-phenanthroline)rhenium(I)] {*fac*-[Re(phen)$(CO)_3$Cl], **1**}. We also report the crystal structure of the ephen ligand.

[a] University of Puerto Rico, Río Piedras,
Department of Chemistry,
P. O. Box 23346, Río Piedras, Puerto Rico, 00931
Fax: (internat.) + 1-787-756-8242
E-mail: jorgecr@caribe.net

Supporting information for this article is available on the WWW under http://www.eurjic.org or from the author.

  DOI: 10.1002/ejic.200400531

Results and Discussion

Crystal Structure Description

The structure of **1** consists of a rhenium(I) atom octahedrally coordinated by a chelating phenanthroline ligand, a chloride ion and three carbonyl groups in a facial conformation (Figure 1 and Supporting Information; for Supporting Informations see also the footnote on the first page of this article). Selected bond lengths and bond angles are listed in Table 1. Although this molecule was prepared by Wrighton et. al ca. 30 years ago, this is the first time that its crystal structure has been reported.

The bond lengths in **1** agree with those in similar *fac*-(tricarbonylrhenium) compounds.[4,8] The average Re−N bond length is 2.179(3) Å which is shorter than the Re−N bond length of 2.211(3) Å for *fac*-[tricarbonyl(chloro)bis-(pyridine)rhenium] [$Re(py)_2(CO)_3Cl$], and 2.218(6) and 2.200(6) Å for *fac*-[tricarbonyl(chloro)bis(4,4′-bipyridine)-rhenium] [$Re(4,4'\text{-bpy})_2(CO)_3Cl$].[9]

Figure 2 shows an ORTEP representation of **2**·$CHCl_3$. The structure of **2**·$CHCl_3$ is similar to that of the parent ligand 1,10-phenanthroline with some evident exceptions (Supporting Information, Figure S1).[10] The insertion of oxygen atoms at positions 5 and 6 of the phenanthroline ligand disrupts the delocalised π-system aromaticity in the ligand. The effect of this disruption is that the two pyridine rings rotate relative to each other by ca. 6° (rotation about the C11−C12 axis).

The X-ray crystal structure of **2**·$CHCl_3$ shows a chloroform solvent molecule hydrogen-bonded to the nitrogen atoms of the ephen ligand. However, this bifurcated hydrogen bond is weak (H···N distances of 2.41 Å and 2.30 Å) and the crystals of **2**·$CHCl_3$ loses the chloroform molecule easily. This type of weak hydrogen bond has been well documented in the literature.[11] Mascal presented statistical evidence of C−H···N hydrogen bonding in a variety of crystal structures with H···N distances ranging from 2.05 to 2.45 Å.[12] An additional hydrogen bond between C1−H and the epoxy oxygen atom of a nearby **2**·$CHCl_3$ molecule (H···O 2.64 Å) adds stability to the crystal lattice (see Supporting Information, Figure S2).

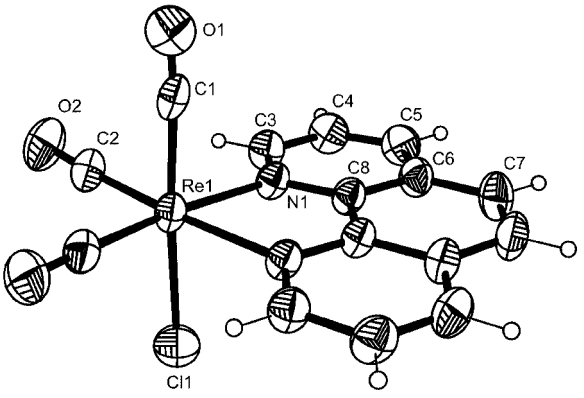

Figure 1. ORTEP representation of **1**; ellipsoids are shown at the 50% probability level

Table 1. Selected bond lengths [Å] and angles [°] for **1**

Re−N1	2.179(3)	Re−C2	1.917(4)
Re−C1	1.973(6)	Re−Cl1	2.4688(17)
N1−Re−N1	75.77(17)	C1−Re−Cl1	176.33(14)
N1−Re−Cl1	84.93(9)	C1−Re−N1	92.18(14)
C2−Re−Cl1	93.79(13)	C2−Re−C2	91.1(3) 6
C2−Re−C1	88.77(16)	Re−C1−O1	176.2(5)
C2−Re−N1	172.33(15)	Re−C2−O2	176.6(4)

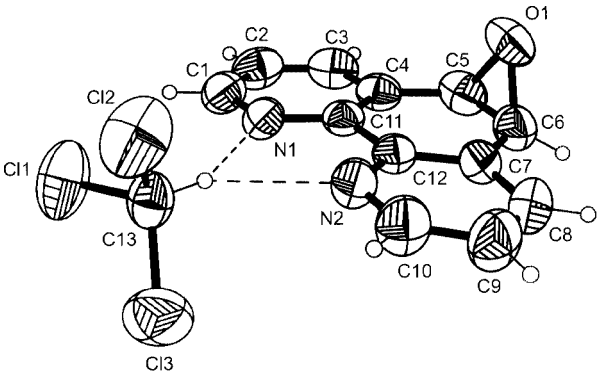

Figure 2. ORTEP representation of **2**·$CHCl_3$; ellipsoids are shown at the 50% probability level

Figure 3 shows an ORTEP representation of **3a**. For *fac*-[$Re(ephen)(CO)_3Cl$] we found two polymorphs, **3a** and **3b**, in which the chloride ion is *trans* to the chloro ligand in both forms (Supporting Information, Figure S1). There are no significant differences between the bond lengths and angles in **3a** and **3b**. The Re atom is in a distorted octahedral environment with the carbonyl groups in a facial arrangement as in the parent compound **1**. The most significant deviation from octahedral geometry can be seen for the chloride ion where C1−Re−Cl1 is 176.58(16)°

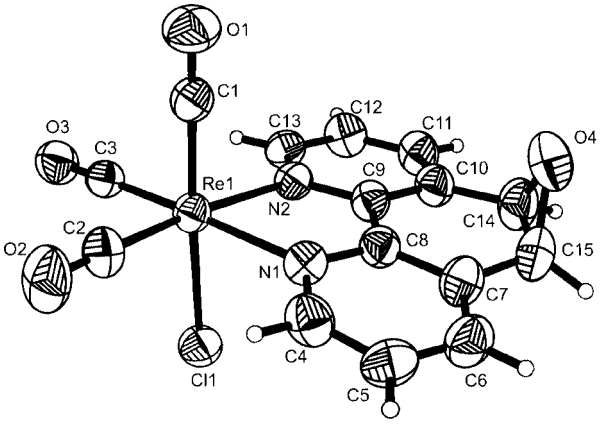

Figure 3. ORTEP representation of **3a**; ellipsoids are shown at the 50% probability level

Table 2. Selected bond lengths [Å] and angles [°] for **3a**

Re−N1	2.172(4)	Re−C3	1.928(5)
Re−N2	2.171(4)	Re−Cl1	2.4600(16)
Re−C1	1.915(6)	O4−C14	1.456(7)
Re−C2	1.918(5)	O4−C15	1.471(8)
N1−Re−N2	75.48(15)	C1−Re−N2	91.87(19)
N1−Re−Cl1	82.18(13)	C1−Re−C2	89.4(2)
N2−Re−Cl1	84.88(11)	Re−C1−O1	179.6(5)
C1−Re−Cl1	176.58(16)	Re−C2−O2	178.8(5)
C2−Re−Cl1	93.64(18)	Re−C3−O3	177.5(4)
C3−Re−Cl1	91.24(13)	C2−Re−C3	88.8(2)
C2−Re−N1	96.89(18)	C14−O4−C15	61.0(4)
C3−Re−N2	98.72(17)	O4−C14−C10	115.5(4)
C1−Re−N1	95.99(19)	O4−C15−C7	114.5(5)

(Table 2). This angle is similar to that of 176.33(14)° in **1**. The bonds lengths and angles are similar to those of **1**, differing only in the ephen ligand. The distinguishing feature between the structures of the polymorphs **3a** and **3b** is the number of weak C−H···O hydrogen bonds (H···O < 2.67 Å) between adjacent molecules of **3a** and **3b**, respectively, with there being one for **3a** and three for **3b** (Supporting Information, Figures S3 and S4).

Infrared Spectroscopy

The IR spectrum of **1** (Figure 4) shows three bands in the 2100−1800 cm^{-1} region which can be attributed to the vibrations of the carbonyl groups in the facial conformation. Group theory predicts that a molecule with C_{3v} point group symmetry must possess two fundamental vibrational modes (both IR- and Raman-active), i.e. an A_1 symmetric stretching mode and a degenerate E stretching mode.[13] Since the symmetry of **3** is C_s, the local C_{3v} symmetry of the carbonyl groups is perturbed. Thus, changing the symmetry from C_{3v} to C_s causes the A_1 mode to become A′ and the degenerate E mode to split into A′ and A″.The carbonyl region of **1** was used to identify the facial isomer and exclude the presence of the meridional isomer.[14] A facial isomer must possess three intense bands in the carbonyl region {e.g., *fac*-[Re(phen)$(CO)_3$Cl] shows three intense bands at 2015, 1912 and 1890 cm^{-1}},[1] while the meridional isomer must possess two intense bands and one weak band at higher wavenumber[15] {e.g., *mer*-[Re$(CO)_3(PPh_3)_2$Cl] shows two intense bands at 1944 and 1894 cm^{-1}, while the weak band expected at ca. 2050 cm^{-1} was not observed}.[16] Figure 4 shows that the IR spectrum of molecule **1** exhibits three intense bands that characterise it as a facial isomer. Staal et al. studied the carbonyl vibrations in analogous complexes [M$(CO)_3$X(DBA)] (M = Mn, Re; X = Cl, Br, I; DBA = 1,4-diazabutadiene) with different substitutions on the DBA ligand.[15] These authors assigned the band above 2000 cm^{-1} to the symmetric stretching mode A′ of the carbonyl groups adjacent to the halogen atom. The next band at higher wavenumber was assigned to the asymmetric A″ mode of the carbonyl groups adjacent to the halogen atom and the last one at the highest wavenumber was assigned to the stretching mode of the carbonyl group *trans* to the halogen atom. Because of the analogy of this system with **1** and **3** we have based our assignment of the vibrational modes on that previous work.

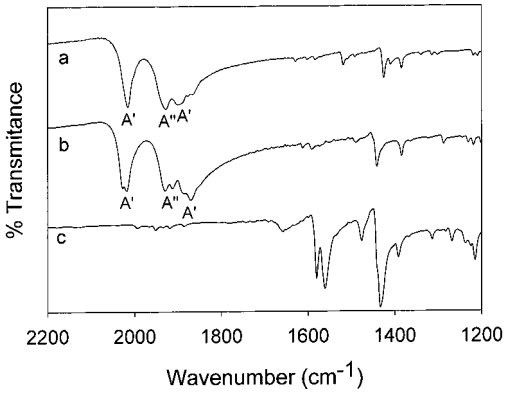

Figure 4. Infrared spectra including the carbonyl region for **1** (a), **3** (crude material) (b) and **2** (c)

In contrast, the spectrum of **3** is more complicated. Each band is split into two (see b in Figure 4), whereas **2** does not show any transition in this region (see c in Figure 4). The splitting of the carbonyl bands observed in the spectrum of **3** will be discussed in the next section along with the NMR spectroscopic results which shed light on the origin of this splitting.

NMR Spectroscopy

^{1}H NMR studies in DMF indicate that **2** possesses three signals in the aromatic region (doublets of doublets) attributable to the pyridine hydrogen atoms (the corresponding atoms in each pyridine ring are equivalent) and an upfield signal attributable to the aliphatic epoxide hydrogen atoms (singlet). ^{13}C NMR spectroscopy shows the signals of the five pyridine carbon atoms in the aromatic region and the epoxide carbon atoms upfield in the hydrocarbon region. These studies confirm that the solution structure of **2** is consistent with its crystal structure (see Supporting Information, Figure S5).

^{1}H NMR spectroscopy of **1** shows four signals in the aromatic region as expected. Six signals in the aromatic region of the ^{13}C NMR spectrum are consistent with the presence of the phenanthroline ligand. The CO carbon signals appear at δ = 190.69 and 198.63 ppm, the latter being assigned to the carbonyl group *trans* to the chloride ion (based on the *trans* effect).

The ^{1}H and ^{13}C NMR spectra of crude **3** are more complicated than would be expected based on the close similarity between **3** and **1** (Figure 5). The most distinctive feature of these spectra compared with those of **1** is that each peak is split. This is especially notable in the ^{13}C NMR spectrum which shows two close sets of resonances when only one is to be expected. Another intriguing finding is that the epoxide resonance in the ^{1}H NMR spectrum (δ = 5.17 ppm) is not split like the rest of the resonances. There are three possible explanations for these observations: (a) there is differentiation of the otherwise equivalent protons of the ephen ligand due to the loss of planarity, (b) there is a mixture of the *fac* and *mer* isomers, or (c) there is a mix-

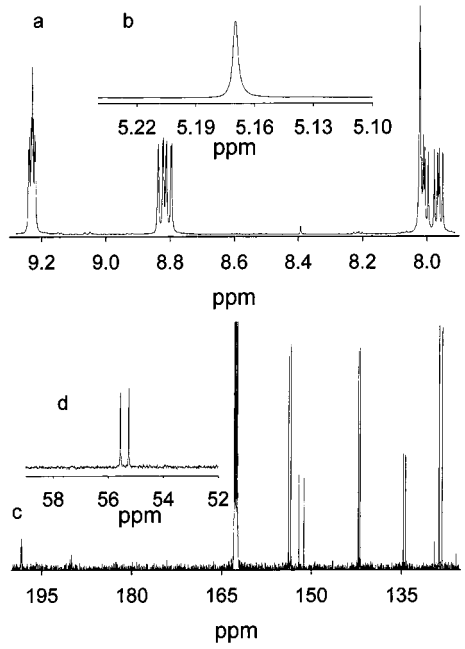

Figure 5. ^{1}H NMR spectrum of **3** (a); ^{1}H NMR high-field ephen hydrogen signals of **3** (crude material) (b); ^{13}C NMR spectrum of **3** (c); ^{13}C NMR high-field ephen carbon signals of **3** (d)

ture of *fac* isomers with the epoxide group of the ephen ligand oriented on different sides of the plane passing through the equatorial carbonyl groups (see Supporting Information, Figure S6).

The first explanation requires that the chemical environment around the protons and carbon atoms on different sides of the mirror plane bisecting the phenanthroline ligand be different enough to show different signals in NMR spectroscopy. The crystal structure shows only subtle differences which can be expected to be normalised by the dynamic environment of the solvent. In addition, this explanation does not account for the splitting of the carbonyl bands in the IR spectra. The splitting of the carbonyl bands appears to be consistent with the existence of two different isomers which leads us to favour either explanation (b) or (c).

In the case of explanation (b), the occurrence of *mer* and *fac* isomers would produce splitting of the bands in the ^{13}C NMR and ^{1}H NMR spectra and the occurrence of new bands in the IR spectroscopic carbonyl region compared with **1**. However, close inspection of the carbonyl region in the ^{13}C NMR spectrum indicates that these resonances are very close to those observed for *fac*-[Re(phen)(CO)$_3$Cl] (**1**). Because the carbonyl groups assume a very different orientation in the *mer* isomer than in the *fac* isomer, one would expect differentiation of the carbonyl signals. However, the spectra suggest that the carbonyl chemical environments of these two isomers are very similar (by the similarity of their carbonyl signals) which is inconsistent with the assignment of a mixture of *fac* and *mer* isomers. Moreover, the synthesis used for **3** is very similar to the one used for **1**, the latter being obtained with a 100% yield of the *fac* isomer.[16] Because of the similarity of these compounds we would expect the synthesis of **3** to also produce only the *fac* isomer. Finally, an octahedral complex with three carbonyl groups in the *fac* conformation would exhibit three intense bands in the carbonyl region (ca. 1900 to 2050 cm^{-1}) while a *mer* isomer must show two intense bands between 2000 and 1900 cm^{-1} and a weak band at ca. 2015 cm^{-1} which on some occasions is even absent.[14,16] As it is evident from Figure 4, the presence of two sets of three intense bands is consistent with the existence of two *fac* isomers.

Explanation (c) requires that the epoxy group has little or no influence on the coordination of the ephen ligand to the rhenium centre. If this is true, it could explain the presence of two closely spaced sets of resonances in both the ^{1}H and ^{13}C NMR spectra and also the observed 1:1 signal intensity ratio. However, only the isomer with the epoxy group *trans* to the chloride ion could be characterised by single-crystal X-ray diffraction. Attempts to crystallise the second isomer were unsuccessful. The structure of the isomer with the epoxy group *trans* to the chloride ion and the proposed structure of the isomer with the epoxy group *cis* to the chloride ion are presented in the Supporting Information (Figure S6).

The unexpected fact that the epoxide proton resonance is not split, prompted us to perform NMR measurements at a higher temperature (60 °C). The most significant difference is the splitting of the epoxide hydrogen resonance at 60 °C (Figure 6) compared with that at 25 °C. These resonances collapse into a single peak when cooled again to 25 °C. Previous studies of this complex at low temperature by Shen and Sullivan indicated that this signal also splits when the material is cooled to −60 °C.[7] This observation led the authors to conclude that a relatively low exchange barrier exists between the *trans* and *cis* isomers. However, the new temperature-dependent data we are presenting indicate that this is not the case. A low isomerisation barrier for this ligand would not produce a splitting of the epoxide signal upon a rise in temperature. Rather, an increase in temperature would increase the rate of isomerisation producing a single peak within the time of measurement of the instrument. Therefore, the appearance of two resonances at 60 °C is consistent with the existence of two *fac* isomers. An explanation could be that the factors which account for the chemical shift of these hydrogen atoms in both isomers cancel out to yield a single resonance at room temperature.

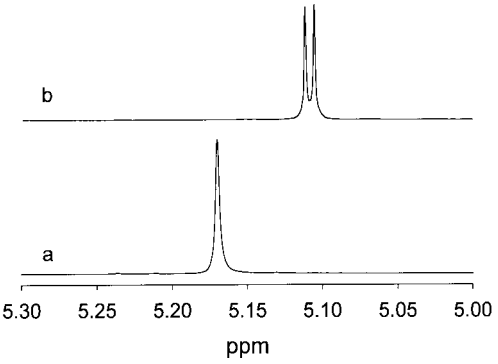

Figure 6. ^{1}H NMR spectrum of crude **3** showing the resonance signals for the hydrogen atoms attributed to the epoxide in the ephen ligand at 25 °C (a) and 60 °C (b)

These coincidental resonances can be differentiated at higher temperature because of the variation of the solvent's physical properties at those temperatures (e.g., density, viscosity, dielectric constant). The other peaks in both the ^{13}C and ^{1}H NMR spectra at 25 °C and 60 °C are very similar, with some minor displacements due to the change in temperature.

Finally, there is still the question of why we observe only one isomer in the crystal structure. We propose that the isomer with the epoxy group *trans* to the chloride ion is preferred during crystallisation because of a more favourable hydrogen bonding network. We also observed that along with the crystals, a yellow powder also precipitates and this could be the other isomer. Infrared spectra of the crystals and the powder (see Supporting Information, Figure S7) correlate exactly except for the carbonyl region which is consistent with the presence of two different isomers. In order to unequivocally assign the NMR spectra of both isomers we determined the ^{1}H NMR spectra of both the crystals and the yellow powder resulting from the recrystallisation of the crude material (see Supporting Information, Figure S8). The ^{1}H NMR spectrum of the crystals exhibit signals which are shifted downfield relative to those of the powder, again supporting our assignment of two different isomers.

Electronic Absorption and Luminescence Characterisation

One of the most distinctive features in the UV/Vis absorption spectrum of **3** is the presence of a peak near 385 nm corresponding to the MLCT band which can be assigned by analogy with its parent compound **1**. As is evident from Figure 7, this band is not present in the spectrum of **2** or that of the phenanthroline ligand (phen). The MLCT absorption maximum of **3** is red-shifted with respect to **1** which suggests that the epoxy oxygen atom draws electron density from the phenanthroline ring, facilitating the photoinduced metal-to-ligand charge transfer.[17]

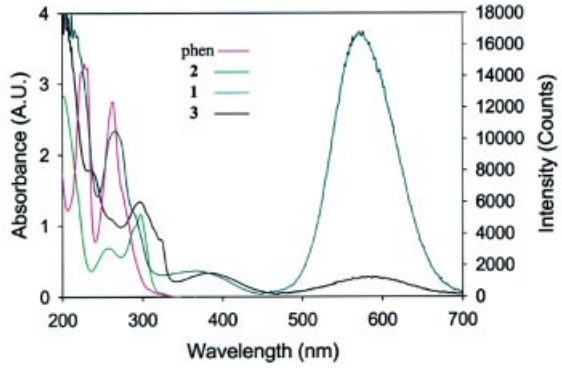

Figure 7. UV/Vis spectra of phen, **2**, **1** and **3**; luminescence spectra are shown for **1** and **3** in the region of 470−700 nm

Studies of **1** by Wrighton et al. indicated that upon absorption this complex undergoes intersystem crossing to the triplet state (or the mixed singlet-triplet state) with nearly 100% efficiency.[1] Luminescence measurements show a red shift in the emission band from 573 nm (**1**) to 585 nm (**3**) as shown in Figure 7.[18] This behaviour is consistent with previous studies using substituted phenanthrolines.[1,19] Quantum yield results (Table 3) indicate that the emission efficiency of **3** is less than that of **1**. In addition, the luminescence lifetime of **3** (15.1 ns) is also less than that of **1** (183 ns). To better understand the relaxation processes of the excited states of these two complexes we determined the radiative and nonradiative decay rate constants. Table 3 shows that the radiative decay rate constants remains basically unaffected while the nonradiative decay rate constant increases by a factor of 10 for **3** compared with that of **1**. Previous studies indicated that the nonradiative decay rate constant is affected by the energy gap.[20] The energy gap law states that the coupling between the vibrational levels of the ground and the excited state increases as the energy gap decreases.[21] A large coupling between the excited- and ground-state vibrational levels will increase the nonradiative decay rate constant. The increase in the nonradiative decay rate constant upon a decrease in the energy gap (as indicated in the red shift from 573 to 585 nm) is consistent with the energy gap law. However, because the aromaticity of the phenanthroline group is affected by the epoxye substitution in positions 5 and 6 a better comparison might be made with [Re(bpy)(CO)$_3$Cl] (**4**) in which the bpy (2,2′-bipyridine) ligand lacks the extensive aromatic delocalisation of phenanthroline. Also, **4** (similar to **3**) displays a lower emission energy and a shorter lifetime than **1**. Table 3 indicates that the energy gap of **3** is smaller than that in **4** while the nonradiative rate constant is larger for **4** than for **3**. The decrease in the energy gap (comparing **3** with **4**) can cause an increase in the coupling between the ground- and excited-state levels increasing the nonradiative pathways and hence the nonradiative rate constant. This behaviour is also consistent with the energy gap law. In addition, the increase in the nonradiative decay rate constant can also be attributed to new deactivation pathways available for the epoxidated phenanthroline ligand in comparison with the unmodified phenanthroline (e.g. thermal deactivation by vibrations of the epoxy oxygen atom and dipole coupling by hydrogen bonds to the epoxide). Tricarbonylrhenium complexes with substituted phenanthrolines like 5-nitro-1,10-phenanthroline and 1,10-phenanthroline-5,6-dione do not exhibit luminescence in dichloromethane at room temperature[1] and this can also be attributed to deactivation pathways due to phenanthroline substitution.

Table 3. Radiative and nonradiative decay rate constant for **1** and **3** in acetonitrile

	Emission $\lambda_{max.}$ [nm]	τ [ns]	φ	k_R [s^{-1}]	k_{NR} [s^{-1}]
1	573	183 ± 5	0.0177	9.67×10^4	5.37×10^6
3	585	15.1 ± 0.8	0.0013	8.61×10^4	6.61×10^7
4	580	25.6 ± 0.9	0.0039	1.56×10^5	3.89×10^7

Conclusion

The crystal structures of *fac*-[Re(phen)(CO)$_3$Cl], ephen and *fac*-[Re(ephen)(CO)$_3$Cl] have been reported. An exten-

sive hydrogen bonding network has been identified in the crystal lattices of **2** and **3**. IR and NMR spectroscopic studies allow the identification of two isomers of **3**. These isomers differ in the orientation of the epoxy oxygen atom relative to the chlorine atom and are nearly equally abundant. Luminescence experiments show an increase in the nonradiative decay rate constant for **3** consistent with the energy gap law. This increase can also arise due to new deactivation pathways available for **3** but not for **1** and **4**. Molecule **3** is potentially useful in synthesising donor-bridge-acceptor systems, photoactive polymers, modified surfaces and a variety of photoactive molecular frameworks involving rhenium centres since the epoxy functionality provides an easy way of forming covalent bonds. The photophysical and structural characterisation of **3** presented in this article is important for the synthesis and study of more complex structures involving this building block. Future studies will include the modification of layered zirconium phosphates using epoxyphenanthroline-based ligands for the covalent attachment of metal complexes to this material.

Experimental Section

Materials: All chemicals were purchased from Aldrich Chemical Co. and used as received. Acetonitrile was of spectrophotometric quality.

Syntheses: The syntheses of *fac*-[Re(phen)$(CO)_3$Cl] (**1**)[1] and ephen (**2**)[7] are described elsewhere. The published procedure for the synthesis of **1** was adopted for the synthesis of *fac*-[Re(ephen)$(CO)_3$Cl] (**3**). In a typical procedure, **2** (0.1068 g) and [Re$(CO)_5$Cl] (0.2001 g) were dissolved in toluene (30 mL). The solution was heated to reflux under N_2 for 1 h and the precipitate obtained was filtered and washed with diethyl ether. The yields were typically ca. 0.2116 g (ca. 80%). ^{1}H NMR of the crude material (DMF, 500 MHz): δ = 5.15 (s, 2 H), 7.97 (m, 2 H), 8.80 (m, 2 H), 9.22 (m, 2 H) ppm. ^{13}C NMR (DMF, 125 MHz): δ = 55.29, 55.59, 128.30, 128.80, 134.40, 134.74, 141.94, 142.21, 151.30, 152.12, 153.46, 153.82, 190.08, 190.31, 198.40, 198.50 ppm.

X-ray Crystal Structure Determinations: Crystals of **1** were grown by slow concentration of a saturated acetonitrile solution at 4 °C. Crystals of **2** were obtained by slow diffusion of hexanes into a saturated chloroform solution. For the crystal structure determination, a crystal of **2**·$CHCl_3$ was sealed in a quartz capillary in order to prevent solvent loss. Two polymorphs of **3** were obtained: **3a** by slow concentration of a saturated acetonitrile solution at 4 °C and **3b** by concentration of a saturated DMF solution at room temperature. X-ray diffraction data, collected from a single crystal in each case mounted atop a glass fibre with a Siemens SMART-CCD diffractometer,[22] were corrected for Lorentz and polarisation effects.[23] The structures were solved by direct methods using the SHELXTL program and refined by full-matrix least-squares methods on F^2.[24] Crystallographic details are summarised in Table 4. CCDC-239409 (**1**), -239410 (**2**), -239411 (**3a**) and -239412 (**3b**) contain the supplementary crystallographic data for this paper. These data can be obtained free of charge at www.ccdc.cam.ac.uk/conts/retrieving.html [or from the Cambridge Crystallographic Data Centre, 12 Union Road, Cambridge CB2 1EZ, UK; Fax: (internat.) + 44-1223-336-033; E-mail: deposit@ccdc.cam.ac.uk].

Spectroscopic Characterisation: UV/Vis absorption measurements were performed with an HP-8453 diode array spectrophotometer. Luminescence measurements were performed with an SE-900 spectrofluorimeter (Photon Technology International, PTI) using a 150-W xenon lamp as the excitation source and a PTI Model 710 photon counting detector with a Hamamatsu R1527P photomultiplier. The bandpass of the emission monochromator was 8.75 nm for the steady-state luminescence experiments at 384 nm and the spectra presented are uncorrected for the photomultiplier efficiency and lamp output. Time domain luminescence measurements were performed using a PTI GL-3300 N_2 pulsed laser coupled with a PTI 5020-ELT stroboscopic detector with a Hamamatsu R1527P photomultiplier. The excitation wavelength was 337 nm while emission was detected at 573 and 585 nm for **1** and **3**, respectively. The iterative reconvolution of the decay transients was performed using PTI Time Master 1.2 software. Quantum yields were determined using [Ru$(bpy)_3$]$(PF_6)_2$ in acetonitrile as a standard (φ = 0.062),[25] using the following formula:[26]

$$\phi = \phi_R \frac{I}{I_R} \frac{OD_R}{OD}$$

Table 4. Crystallographic data for **1**, **2**·$CHCl_3$, and **3**

	1	**2**·$CHCl_3$	**3a**	**3b**
Empirical formula	$C_{15}H_8ClN_2O_3Re$	$C_{13}H_9Cl_3N_2O$	$C_{15}H_8ClN_2O_4Re$	$C_{15}H_8ClN_2O_4Re$
Formula mass	485.88	315.57	501.88	501.88
Space group	*C*2/*m* (No. 12)	*Pbca* (No. 61)	$Pca2_1$ (No. 29)	$P2_1/n$ (No. 14)
a [Å]	15.8686(19)	12.146(3)	15.812(2)	8.2761(11)
b [Å]	11.8859(14)	11.619(2)	10.4330(15)	12.7831(18)
c [Å]	8.0134(10)	19.741(4)	9.1023(13)	13.9959(19)
β [°]	107.154(2)	90	90	92.197(2)
V [Å^3]	1444.2(3)	2785.8(10)	1501.6(4)	1479.6(3)
Z	4	8	4	4
$\rho_{calcd.}$ [g/cm^{-3}]	2.235	1.505	2.220	2.253
μ [mm^{-1}]	8.612	0.649	8.291	8.414
$R1$[a], $wR2$[b] [$I > 2\sigma(I)$]	0.0231, 0.0584	0.0458, 0.0992	0.0177, 0.0445	0.0185, 0.0476
$R1$[a], $wR2$[b] (all data)	0.0243, 0.0591	0.0753, 0.1123	0.0190, 0.0452	0.0209, 0.0489
Goodness-of-fit	1.094	1.019	1.073	1.083

[a] $R_1 = \Sigma||F_o| - |F_c||/\Sigma|F_o|$. [b] $wR_2 = [\Sigma w(F_o^2 - F_c^2)^2/\Sigma w(F_o^2)^2]^{1/2}$.

where φ_R is the quantum yield of the reference standard, I and I_R are the integrated intensities for the luminescent molecule and the standard, respectively. OD and OD_R are the optical densities for the luminescent molecule and the standard solution, respectively. Both quantum yield and lifetime measurements were performed in solutions purged with N_2 (99.9%) for 15 min. Knowledge of the quantum yield and luminescence lifetime allows the determination of the radiative and nonradiative rate constants as follows:

$$k_r = \frac{\phi}{\tau}$$

$$k_{nr} = \frac{(1-\phi)}{\tau}$$

NMR experiments were performed in [D_6]DMF with a Bruker-Advance DRX-500 spectrometer. IR spectra were recorded in KBr pellets with a Nicolet Magna 750 FTIR spectrometer or directly on the sample with a Bruker Tensor 27 FTIR spectrometer.

Acknowledgments

We thank Joe Martinez for his help with the NMR measurements and Dr. Antonio Prieto for helpful discussions. A. A. M. acknowledges NIH-RISE (grant R25GM061151) and NSF Graduate Teaching Fellows in K-12 Education (Award 9979566) for financial support.

[1] M. Wrighton, D. L. Morse, *J. Am. Chem. Soc.* **1974**, *96*, 998−1003.
[2] [2a] P. A. Mabrouk, M. S. Wrighton, *Chem. Phys. Lett.* **1984**, *103*, 332−335. [2b] P. J. Giordano, M. S. Wrighton, *J. Am. Chem. Soc.* **1979**, *101*, 2888−2897. [2c] Y. Yang, J. Chen, Y. Lin, M. Cheng, Y. Wang, *J. Organomet. Chem.* **1994**, *467*, C6−C8.
[3] [3a] S. Sun, D. T. Tran, O. S. Odongo, A. J. Lees, *Inorg. Chem.* **2002**, *41*, 132−135. [3b] S. Sun, A. S. Silva, I. M. Brinn, A. J. Lees, *Inorg. Chem.* **2000**, *39*, 1344−1345. [3c] J. A. Baiano, D. L. Carlson, G. M. Wolosh, D. E. DeJesus, C. F. Knowles, E. G. Szabo, W. R. Murphy, *Inorg. Chem.* **1990**, *29*, 2327−2332.
[4] [4a] W. B. Connick, A. J. Di Billio, W. P. Schaefer, H. B. Gray, *Acta Crystallogr., Sect. B* **1999**, *55*, 913−916. [4b] W. B. Connick, A. J. Di Billio, M. G. Hill, J. R. Winkler, H. B. Gray, *Inorg. Chim. Acta* **1995**, *240*, 169−173.
[5] M. Wrighton, *Chem. Rev.* **1974**, *74*, 401−429.
[6] W. K. Smothers, M. S. Wrighton, *J. Am. Chem. Soc.* **1983**, *105*, 1067−1069.
[7] Y. Shen, P. Sullivan, *Inorg. Chem.* **1995**, *34*, 6235−6236.
[8] [8a] O. S. Wenger, L. M. Henling, M. W. Day, J. R. Winkler, H. B. Gray, *Inorg. Chem.* **2004**, *43*, 2043−2048. [8b] M. Bakir, *Acta Crystallogr., Sect. B* **2002**, *58*, m74−m76. [8c] K. Wang, L. Huang, L. Gao, C. Huang, *Inorg. Chem.* **2002**, *41*, 3353−3358. [8d] D. H. Gilbson, B. A. Sleadd, A. Vij, *J. Chem. Crystallogr.* **1999**, *29*, 619−622. [8e] R. N. Dominey, B. Hauser, J. Hubbard, J. Dunham, *Inorg. Chem.* **1991**, *30*, 4754−4758.
[9] S. Belanger, J. T. Hupp, C. L. Stern, *Acta Crystallogr., Sect. B* **1998**, *54*, 1596−1600.
[10] S. Nishigaki, H. Yoshioka, K. Nakatsu, *Acta Crystallogr., Sect. B* **1978**, *34*, 875−879.
[11] [11a] A. N. M. M. Rahman, R. Bishop, D. C. Craig, M. L. Scudder, *Eur. J. Org. Chem.* **2003**, 72−81. [11b] G. R. Desiraju, T. Steiner, *The Weak Hydrogen Bond*, Oxford University Press, New York, **1999**, p. 4. [11c] G. A. Jeffrey, *An Introduction to Hydrogen Bond*, Oxford University Press, New York, **1997**, chapter 5. [11d]F. H. Allen, J. A. K. Howard, V. J. Hoy, G. R. Desiraju, D. S. Reddy, C. C. Wilson, *J. Am. Chem. Soc.* **1996**, *118*, 4081−4084. [11e] T. Steiner, J. A. Kanters, J. Kroon, *Chem. Commun.* **1996**, 1277−1278. [11f] G. P. A. Yap, A. L. Rheingold, P. Das, R. H. Crabtree, *Inorg. Chem.* **1995**, *34*, 3474−3476. [11g] P. Behrens, G. van de Goor, C. C. Freyhardt, *Angew. Chem. Int. Ed. Engl.* **1995**, *34*, 2680−2682. [11h] T. Steiner, *Chem. Commun.* **1994**, 2341−2342.
[12] M. Mascal, *Chem. Commun.* **1998**, 303−304.
[13] F. A. Cotton, *Chemical Applications of Group Theory*, John Wiley & Sons, New York, **1990**, chapter 10.
[14] B. J. Brisdon, D. A. Edwards, J. W. White, *J. Organomet. Chem.* **1978**, *156*, 427−437.
[15] L. H. Staal, A. Oskam, K. Vrieze, *J. Organomet. Chem.* **1979**, *170*, 235−245.
[16] A. M. Bond, R. Colton, M. E. McDonald, *Inorg. Chem.* **1978**, *17*, 2842−2847.
[17] H. Kunley, A. Vogler, *Inorg. Chim. Acta* **2003**, *343*, 357−360.
[18] The luminescence spectra for the tricarbonylrhenium complexes are uncorrected. Although the $\lambda_{max.}$ values are blue-shifted compared with previously reported values using corrected spectra (K. Kalyanasundaram, *Inorg. Chem. Commun.* **2000**, *188*, 323) we are only comparing uncorrected spectra recorded in our laboratory under different chemical micro-environments.
[19] D. R. Striplin, G. A. Crosby, *Coord. Chem. Rev.* **2001**, *211*, 163−175.
[20] J. V. Caspar, T. J. Meyer, *J. Phys. Chem.* **1983**, *87*, 952−957.
[21] T. J. Meyer, *Pure Appl. Chem.* **1986**, *58*, 1193−1206.
[22] Data Collection: *SMART-NT Software Reference Manual*, version 5.0, Bruker AXS, Inc., Madison, WI 53719-1173, **1998**.
[23] Data Reduction: *SAINT-NT Software Reference Manual*, version 4.0, Bruker AXS, Inc., Madison, WI 53719-1173, **1996**.
[24] G. M. Sheldrick, *SHELXTL-NT*, version 5.1, Bruker AXS, Inc., Madison, WI 53719-1173, **1999**.
[25] R. Alarcon, *Synthesis and characterisation of Re^{I} complexes used for protein modification and intercalation in zirconium layered materials*, Masters Degree, University of Puerto Rico, Río Piedras P.R., February **1997**, p. 62.
[26] [26a] J. R. Lakowicz, *Principles of Fluorescence Spectroscopy*, Kluwer Academics/Plenum Publisher, New York, **1999**, pp. 52−53. [26b] C. A. Parker, W. T. Rees, *Analyst (Cambridge, U. K.)* **1960**, *85*, 587−600.

Received June 17, 2004
Early View Article
Published Online November 10, 2004
Minor changes have been made to the manuscript since it's publication in *Eur. J. Inorg. Chem.* Early View. *The Editors*